MODELLING INTERFERENCE BETWEEN THE GEOGRID BEARING MEMBERS UNDER PULLOUT LOADING CONDITIONS

G. Cardile[1], D. Gioffrè[2], N. Moraci[3] and L.S. Calvarano[4]

[1] Assistant Professor of Geotechnical Engineering, Ph.D. — *Mediterranea* University of Reggio Calabria, Department of Civil Engineering, Energy, Environment and Materials (DICEAM), Italy- Telephone: +39 0965 169 2213; Telefax: +39 0965 1692201, e-mail: giuseppe.cardile@unirc.it (corresponding authors)

[2] Assistant Professor of Geotechnical Engineering, Ph.D. — *Mediterranea* University of Reggio Calabria, Department of Civil Engineering, Energy, Environment and Materials (DICEAM), Italy- Telephone: +39 0965 169 2213; Telefax: +39 0965 1692201, e-mail: domenico.gioffre@unirc.it

[3] Full Professor of Geotechnical Engineering, Ph.D. — *Mediterranea* University of Reggio Calabria, Department of Civil Engineering, Energy, Environment and Materials (DICEAM), Italy- Telephone: +39 0965 169 2263; Telefax: +39 0965 1692201, e-mail: nicola.moraci@unirc.it

[4] Research Assistant in Geotechnical Engineer, Ph.D. — *Mediterranea* University of Reggio Calabria, Department of Civil Engineering, Energy, Environment and Materials (DICEAM), Italy- Telephone: +39 0965 169 2306; Telefax: +39 0965 1692201, e-mail: lidia.calvarano@unirc.it

ABSTRACT

The main interaction mechanisms affecting the pullout resistance of geogrids embedded in soils are the skin friction between soil and reinforcement solid surface and the bearing resistance which develops against transversal elements. As regards bearing resistance the interference mechanism plays an important role: this can occur when the spacing between transversal members is lower than a threshold value, depending on the extensions of active and passive surfaces mobilized on bearing members.

Based on the result of several large-scale pullout tests, a theoretical method to determine the peak pullout resistance of extruded geogrids embedded in a compacted granular soil is proposed. The method takes into account the interference mechanism due to the

proximity of the transversal bearing members and works well for soil-geogrid interfaces in which scale effect is negligible.

KEYWORDS: Geosynthetics, geogrids, theoretical model, pullout resistance, interaction mechanisms, interference.

1 INTRODUCTION

To model the behaviour of GRS structures using numerical methods requires knowledge of the constitutive model that should be adopted for reinforcement and soil, along with definition of the interface model. Therefore, it is essential to define the stress–strain–time relationships of the system's constituent parts (Cardile et al., 2016b; Perkins, 2000) and to model the behaviour of the soil-geosynthetic interface while taking into account the complex mechanisms of interaction. A thorough understanding of these mechanisms could allow the production of geosynthetic reinforcements, optimizing costs and performance (Bathurst and Ezzein, 2015b; Calvarano et al., 2014; Esfandiari and Selamat, 2012; Ferreira et al., 2015; Hatami and Esmaili, 2015; Liu et al., 2009; Liu et al., 2016; Moraci and Cardile, 2008; Moraci and Cardile, 2009, 2012; Moraci and Recalcati, 2006; Mosallanezhad et al., 2016; Pinho-Lopes et al., 2016; Sieira et al., 2009; Suksiripattanapong et al., 2013; Tran et al., 2013; Vangla and Gali, 2016; Vieira et al., 2013; Wang et al., 2014; Wang et al., 2016).

The soil geosynthetic interaction can be very complex. Direct shear tests and pullout tests can simulate both mechanisms in laboratory, using large size devices.

For soil-geotextile interfaces the only mechanism that develops is the skin friction, while for soil-geogrid interfaces the interaction becomes more complex due to the open structure of this type of geosynthetic. The main interaction mechanisms concerning pullout resistance of extruded geogrids embedded in compacted soil are the skin friction between soil and reinforcement solid surface and the bearing resistance that develops against transversal members (Jacobs et al., 2014; Moraci et al., 2007; Moraci et al., 2014a; Moraci and Gioffrè, 2006; Palmeira, 2009; Ziegler and Timmers, 2004).

Therefore, the ultimate pullout resistance of geogrids has been typically interpreted as the sum of the passive and interface shear components (Jewell, 1996):

$$P_R = P_{RS} + P_{RB} \tag{1}$$

where P_{RS} is the skin friction component of pullout resistance and P_{RB} is the bearing component of pullout resistance.

Generally, the two components are assumed to be independent of each other when it should be considered that one mechanism of interaction affects the other to an extent not yet well understood or quantified.

The first term on the right-hand side of equation (1), for a geogrid of length L_R and unit width W_R (Figure 1), may be evaluated using the following expression:

$$P_{RS} = 2\alpha_S L_R \tau = 2\alpha_S L_R \sigma'_n \tan\delta \tag{2}$$

where σ_n' is the effective normal stress; δ is the skin friction angle between soil and geogrid; τ is the shear stress acting at soil-reinforcement interface; α_S is the fraction of geogrid surface area that is solid.

According to Jewell (1990), the bearing component of pullout resistance can be evaluated as follows:

$$P_{RB} = \left(\frac{L_R}{S}\right)\alpha_B \sigma'_b B \tag{3}$$

where S is the spacing between the geogrid bearing members; L_R/S is the number of geogrid bearing members; α_B is the fraction of total frontal area of geogrid available for bearing resistance; B is the thickness of the bearing members; σ'_b is the effective bearing stress mobilizing on geogrid bearing members.

To evaluate the bearing stress σ'$_b$, different failure mechanisms can be used. Jewell et al. (1985) used a punching failure mechanism (lower bound); Peterson and Anderson (1980) used a general shear failure (upper bound); Bergado and Chai (1994) used a modified punch-ing mechanism; Matsui et al. (1996) used a Prandtl failure mechanism. For granular soils, the bearing stresses σ'$_b$ acting on geogrid bearing members depend on soil shear strength angle, initial stress state, interface roughness and reinforcement depth in relation to the sizes of the bearing members. In spite of this, in the equations proposed by the different authors, the ratio σ'_b/σ'_n only depends on soil shear angle. Therefore, the pullout resistance of a geogrid is:

$$P_R = 2 \cdot \alpha_S \cdot L_R \cdot \sigma_n^{'} \cdot \tan\delta + \left(\frac{L_R}{S}\right) \cdot \alpha_B \cdot B \cdot \sigma_b^{'} = 2 \cdot f_b \cdot L_R \cdot \sigma_n^{'} \cdot \tan\phi' \qquad (4)$$

where f_b is the interaction coefficient under pullout loading conditions.

The coefficient f_b can be obtained as a function of reinforcement geometrical parameters (α_s, α_b, B, S), soil shear strength angle (ϕ'), soil-geosynthetic skin friction angle (δ), and effective stresses acting at the interfaces (σ'_n, σ'_b):

$$f_b = \alpha_S \cdot \left(\frac{\tan\delta}{\tan\phi^{'}}\right) + \left(\frac{\alpha_b \cdot B}{S}\right)^{'} \cdot \left(\frac{\sigma_b^{'}}{\sigma_n^{'}}\right) \cdot \frac{1}{2 \cdot \tan\phi^{'}} \qquad (5)$$

In the theoretical equation (5), there are two components representing both skin friction and bearing interaction.

The interference phenomenon for closely spaced bearing members S (i.e. for small value of the ratio between S and the thickness of transverse ribs B_{eq}) plays an important role in the mobilisation of the bearing resistance. To be more precise, a significant part of the surface of the longitudinal members of the reinforcement is involved in this phenomenon, suggesting that under similar conditions the skin friction (for geogrids it generally represents less than 20% of the pullout resistance) also decreases.

Some researchers (Bergado et al., 1993; Dyer, 1985; Jewell, 1996; Milligan et al., 1990; Palmeira, 2004, 2009; Palmeira and Milligan, 1989) found that the bearing resistance also depends on the ratio between the thickness of transverse rib B_{eq} and the soil mean particle size D_{50} (i.e. scale effect) and on the shape of the transverse rib.

2 INTERFERENCE MECHANISM FOR CLOSELY SPACED BEARING MEMBERS

When pullout-loading acts on the soil-geosynthetic system the mobilisation of soil passive resistance developed in front of the bearing surface of transversal rib causes a stress increase and causes rotation of the principal stresses (Palmeira, 2004). The pullout displacement of the geogrid implicates that behind each transversal rib the stress decreases forming a disturbed region (softened region), which will affect the maximum bearing strength developed along the following bearing members if they are too close to each other.

Recently, different researchers have analysed the behaviour at the interface using a micro-image analysis system (Bathurst and Ezzein, 2015a, b; Ezzein and Bathurst, 2014; Zhou et al., 2012). The novel combination of technologies allows the measuring of the complete displacement field of reinforcement and/or target particles seeded in the surrounding soil during pullout tests. Zhou et al. (2012), using micro-image analysis captured the interaction mechanisms between sand and the transverse ribs of reinforcement: the geogrid was located close to the glass side wall, so that it might be captured. In order to clarify the interaction mechanisms between sand and geogrid

transversal members Zhou et al. (2012) carried out pullout tests at confining pressure equal to 30 kPa on HDPE geogrid ($J_{2\%}$=13.5 kN/m; S=39 mm; B_{eq}=2.28 mm) embedded in compacted soil (D_{50}=0.38 and D_R=0.66) which they analysed using a particle image velocimetry technology. During the pullout tests, sand motion around geogrid ribs was captured with a micro-images analysis system. Figure 2 shows particle motion around a transverse rib above and below the interface at various stages: sand particles which are located ahead of the transverse rib rotate during pullout, the particles above the longitudinal geogrid axis rotate in a clockwise direction while particles on the lower of the longitudinal axis rotate anticlockwise. Particles on the top right side of the transverse rib fall into the voids created during the movement of the geogrid (in the softened region). The micro-image analysis confirms that the soil located in front of the transverse rib is subjected to a passive state of stress while behind it an active state is reached, creating a loose soil region. Sand particles do not move symmetrically along the interface (above and below the longitudinal axis of the geogrid) due to the different boundary conditions. Finally, for the specific test boundary conditions adopted in the research it was possible to observe that, at 30 kPa and 10 mm pullout displacement, the average thickness of passive failure surface was approximately equal to six times the rib thickness and its length was about ten times the rib thickness (Moraci et al., 2014a).
Previously researches (Palmeira, 2009) have shown that, for a fixed equivalent bearing member thickness B_{eq}, the lower the spacing S between two consecutive transversal ribs, the greater will be the reduction in strength due to interference phenomenon. Moreover, interference is controlled by bearing member thickness B_{eq} also through the ratio with soil particle diameter (B_{eq}/D_{50}). The minimum ratio S/B_{eq} above which this phenomenon affects pullout behaviour, decreases with increasing B_{eq}/D_{50} ratio (Sukmak

et al., 2015). In more detail, the decreasing of D_{50} causes a reduction in the soil shear strength affecting the softened region and the failure plane (shape and size) developed ahead of the transverse members.

Using photo-elastic studies on a steel grid, Dyer (1985) and Milligan et al. (1990) clearly showed the interaction between transversal bearing members of the grid and the surrounding soil. Passive load distribution between transverse members is uniform only if the members are sufficiently distant from one another. In order to investigate this topic, Palmeira (1987) carried out pullout tests at low normal vertical stress (σ'_n=25 kPa) by using single isolated bearing members and metal grids (B varying from 1.5 and 4.78 mm) with different geometric characteristics (S=18 mm, 62 mm and 129 mm - friction along the longitudinal ribs was minimized through the application of grease) in dense sands (D_{50}=0.4, 0.8 and 1.6 mm). The tests results showed that the S/B ratio above which grid-bearing members behaved as in isolation was greater than 40-50, for the adopted testing conditions (confining pressure, geotechnical characteristic of the soils and geometrical and mechanical characteristic of the reinforcements).

The above researchers carried out different pullout tests varying the ratio B_{eq}/D_{50}: increasing this value, the observed failure mechanism changes from the punching shear to a generalized one. For these testing boundary conditions, when the ratio exceeds 7-12, the bearing strength starts to become independent of the soil particle size.

Experimental evidence provided by Cazzuffi et al. (2011) showed the existence of an optimum spacing between the transversal ribs, which maximizes the peak pullout resistance. In order to study the interference phenomenon, the authors performed a series of pullout tests (in the same testing conditions) on specimens of the same geogrid, characterized by different spacing between the bearing members obtained by removing some transversal ribs (maintaining only the nodes) from the virgin specimen. When the distance between transverse members S is below the "optimum" value, the pullout response appears to be unfavourably affected by the interference phenomenon. On the other hand, when S is above the "optimum" value, the pullout resistance decreases because of the lower number of bearing members that provide the passive resistance contribution to the overall pullout resistance.

3 MODELLING OF SOIL–GEOSYNTHETIC INTERACTION IN PULL-OUT TESTS

Moraci and Gioffrè (2006) proposed a simple theoretical method to predict the peak pullout resistance of extruded geogrids embedded in compacted granular soils that can be used where scale and interference effects are both negligible. This method takes into account the non-linearity in the failure envelope of compacted granular soil (due to the dilatancy effect) as well as the extensibility of reinforcements. The method was based on the evaluation of both frictional and bearing components of pullout resistance using the following equation:

$$P_R = 2 \cdot C_{\alpha S} \cdot \alpha_S \cdot L_R \cdot \sigma_n^{'} \cdot \tan\delta + n_t \cdot n_{tb} \cdot A_b \cdot \sigma_b^{'} \qquad (6)$$

where: $C_{\alpha S}$ = reduction coefficient of geogrid area where skin friction develops; δ = mobilized skin friction angle between soil and geogrid depending on soil dilatancy and reinforcement extensibility; $n_t = L_R/S$ = number of geogrid bearing members; n_{tb} = number of nodes in a transversal element; $A_b = A_t + A_r$ = area of each rib element (including the single node and the bar portion between two nodes) where the bearing resistance can be mobilized; σ'_b = bearing stress.

Moreover, the complex geometry of transverse bars was assumed to be equivalent to that of a strip of uniform thickness B_{eq}.

The bearing stress σ'_b was evaluated using the equation proposed by Matsui et al. (1996) on a Prandtl's local failure mechanism:

$$\frac{\sigma_b^{'}}{\sigma_n^{'}} = e^{\pi tan\phi} tan\left(\frac{\pi}{4}+\frac{\phi'}{2}\right)\left[cos\left(\frac{\pi}{4}-\frac{\phi'}{2}\right)+\left(1-sin\varphi^{'}\right)sin\left(\frac{\pi}{4}-\frac{\phi'}{2}\right)\right] \quad (7)$$

where the symbols stand for: σ'_n= normal effective stress; ϕ'= soil shear strength angle. On the basis of the pullout test results obtained in previous researches (Cardile et al., 2014; Cardile et al., 2016a; Cazzuffi et al., 2014; Moraci et al., 2014b), an upgrade of the theoretical method developed by Moraci and Gioffrè (2006) is herein proposed. The new method, aimed to determine the peak pullout resistance of extruded geogrids embedded in a compacted granular soil (in which scale effects are negligible), takes into account the interference mechanism modelled by introducing a reduction factor $C_{\alpha b}$, on the passive component of the pullout resistance P_{RB}:

$$P_R = 2 \cdot C_{\alpha S} \cdot \alpha_S \cdot L_R \cdot \sigma_n^{'} \cdot \tan\delta + C_{\alpha b} \cdot n_t \cdot n_{tb} \cdot A_b \cdot \sigma_b^{'} \quad (8)$$

The equation of the reduction factor $C_{\alpha b}$, which is a function of the geometrical characteristics of the mesh reinforcement (ratio S/B_{eq}) and of the normal effective stress σ'_n, will be defined in the following sections.

3.1 EXPERIMENTAL DATABASE

The experimental results of several pullout tests performed in previous researches (Cardile et al., 2014; Cardile et al., 2016a; Cazzuffi et al., 2014; Moraci et al., 2014b) using large-scale pullout equipment (Moraci and Cardile, 2009, 2012; Moraci and Recalcati, 2006) has been analysed in this paper.

Pullout tests were carried out on four different PP biaxial geogrids tested in machine and transversal direction (referred to as GGR1, GGR2, GGR3, GGR4) and three HDPE uniaxial extruded geogrids (referred to as GGR5, GGR6, GGR7) embedded in two compacted granular soils (initial unit weight corresponding to 95% of γ_{dmax}). In Table *1* the geometrical characterization of the geogrids used in the research are summarised. All the geogrids showed a different number of tensile elements per unit width, different transversal rib spacing and different cross sectional shape, where the main differences are in rib thickness. The passive interaction mechanisms develop both at the node embossments and at the transversal ribs. Therefore, geogrids geometry was carefully determined to calculate the effective passive resistance surfaces. Figure *3* shows a schematic cross section of a generic bearing member that is placed transversely to the direction of pullout force. The complex geometry of the bearing member (transverse rib), including the areas A_b in the same transverse element, was assumed to be equivalent to that of a strip of uniform thickness (B_{eq}).

The first soil (referred to as Soil A) was a uniform medium sand (SP according to USCS classification system). The sand has a grain shape from sub-rounded to rounded, uniformity coefficient U equal to 1.96, and average grain size D_{50} equal to 0.32 mm. Standard Proctor compaction tests results provide a maximum dry unit weight γ_{dmax} =16.24 kN/m^3 at an "optimum" water content w_{opt} =13.5%.

The second soil (referred to as Soil B) was classified as sand with gravel (SW according to USCS classification system, A1-b according to CNR-UNI 10006 classification system), with a grain shape from sub-rounded to rounded, uniformity coefficient, U, equal to 7.48, and average grain size, D50, equal to 1.47 mm. The Standard Proctor compaction tests performed on Soil B indicates a maximum dry unit weight, γ_{dmax} =18.36 kN/m^3, at an "optimum" water content w_{opt} =9.8%.

Table *2* shows in detail the peak and constant volume shear strength angles of the soils used in the tests. These results were obtained by means of direct shear tests carried out at an initial unit weight corresponding to 95% of γ_{max} at different normal effective stress (σ'_n =10, 25 50 and 100 kPa).

The pullout tests were carried out varying, for each geogrid, the specimen length (L_R equal to 0.40 m, 0.90 m and 1.15 m) and the applied normal effective stress (σ'_n equal to 10 kPa, 25 kPa and 50 kPa). All pullout tests described herein were performed at controlled rates of displacement (CRD) equal to 1.0 mm/min, until geogrid tensile failure or until a total horizontal displacement of 100 mm was reached.

In order to carry out an analytical study on scale effects based on experimental results, it is necessary to select geogrids for which the interference effects are negligible. Table *1* reports the ratio S/B_{eq} values of all experimental geogrids database. It can be observed that only the uniaxial geogrids (GGR5, GGR6, GGR7) have a ratio S/B_{eq} higher than 50. Therefore, according to Palmeira (2009), the pullout results for these soil-geogrids interfaces are not affected by interference effects while scale effects could be possible depending on ratio B_{eq}/D_{50}.

Referring to the three uniaxial HDPE geogrids (GGR5, GGR6, GGR7), which are not subject to interference phenomenon, the authors obtained the values of bearing stress σ'_b from the experimental peak value of pullout resistance P_R^{Exp} with the method proposed by Moraci and Gioffrè (2006) using the following expression:

$$\sigma_b'^{Exp} = \frac{P_R^{Exp} - 2\alpha_S L_R \sigma_n' \tan\delta}{n_t n_{tb} A_b} \qquad (9)$$

Figure *4*a shows the normalised bearing stress σ'^{EXP}_b /(σ'_n tan ϕ') plotted against the bearing member thickness normalised by the average grain size of the soils B_{eq}/D_{50}. In order to plot the results for the different compacted granular soils, the stress ratio $\sigma'_b{}^{EXP}/\sigma'_n$ is normalised by the tangent of the soil shear strength angle taking into account the non-linearity of the envelope of rupture of the different fill soils (effect due to the dilatancy of the soils).

The results show that the normalised bearing strength starts to become independent of the average grain size of the soils only for ratios B_{eq}/D_{50} above 10.

Regarding the four PP biaxial geogrids with similar ratio S/B_{eq}, in which the interference phenomena are not negligible, the same threshold B_{eq}/D_{50} value was obtained (Figure *4*b). However, due to the interference effect, the values of normalised bearing stress are lower than those of uniaxial geogrids.

Therefore, in order to evaluate an analytical equation of interference coefficient $C_{\alpha b}$, the analysis focused on geogrids with ratios B_{eq}/D_{50} above 10 (scale effect negligible) in which the interference effect affected the interaction mechanism of pullout resistance (S/B_{eq} <50).

Figure *5* shows the pullout curves for the selected geogrids (GGR1, GGR2, GGR3 and GGR4) varying the normal effective confining stress for each anchorage length. Due to interference phenomena for closely spaced bearing members, experimental data show comparable values of the peak pullout resistance even though the bearing area of the geogrids ($n_t\, n_{tb}\, A_b$) are very different.

4 PROPOSED ANALYTICAL METHOD

The analytical method proposed by Moraci and Gioffrè (2006) was improved by taking into account the interference effect using the reduction factor for the bearing resistance $C_{\alpha b}$, according to the equation (8). The evaluation of $C_{\alpha b}$ was obtained using the following approach.

The theoretical skin friction component of pullout resistance P_{RS}^{Theor} was evaluated neglecting the interference effect on the skin friction component of pullout resistance ($C_{\alpha S} = 1$), using the following equation:

$$P_{RS}^{Theor} = 2 C_{\alpha S} \alpha_S L_R \sigma_n' \tan\delta = 2 \alpha_S L_R \sigma_n' \tan\delta \qquad (10)$$

where the skin friction angle δ between soil and geogrid was determined by means of previous experimental tests on smooth geomembranes, performed at the same confined pressure used in this research and assumed equal to 1/3 ϕ' (Fannin and Raju, 1993; Moraci and Gioffrè, 2006; Raju, 1995).

The experimental bearing component of pullout resistance was evaluated as:

$$P_{RB}^{Exp} = P_{R}^{Exp} - P_{RS}^{Theor} \qquad (11)$$

where P_R^{Exp} is the experimental peak pullout resistance.

Finally, the interference reduction factor for the bearing resistance $C_{\alpha b}$ can be given as follows:

$$C_{\alpha b} = \frac{P_{RB}^{Exp}}{P_{RB}^{Theor}} = \frac{P_{R}^{Exp} - P_{RS}^{Theor}}{P_{RB}^{Theor}} = \frac{P_{R}^{Exp} - P_{RS}^{Theor}}{n_t n_{tb} A_b \sigma_b'} \qquad (12)$$

Generally, extensibility induces a progressive mobilization of the frictional and passive mechanisms. In order to take into account the reinforcement extensibility and the non-linear failure envelope for the backfill soil (due to dilatancy effects), skin friction was evaluated using an average value of the shear strength angle between the peak and the constant volume values, and the bearing resistance component of pullout resistance was evaluated using the peak shear strength angles corresponding to the different vertical effective stresses.

Figure 6 shows the interference reduction factors $C_{\alpha b}$ obtained by equation (12) versus the ratio S/B_{eq}. The experimental points for each selected geogrid refer to the average value obtained by varying anchorage length L_R. Due to the low variability of the results obtained by varying vertical normal stress σ'_n, a linear regression was fitted. When the ratio S/B_{eq}>50, interference phenomenon can be considered negligible (GGR5, GGR6 and GGR7 in Figure 6), then interference reduction factor $C_{\alpha b}$ is equal to one.

Therefore, it is possible to evaluate the interference reduction factor $C_{\alpha b}$ as follows:

$$C_{\alpha b} = \begin{cases} a \cdot \dfrac{S}{B_{eq}} & \dfrac{S}{B_{eq}} \leq 50 \\ 1 & \dfrac{S}{B_{eq}} > 50 \end{cases} \qquad (13)$$

Where the constant coefficient *a* obtained by linear regression is equal to 0,02.

Hence, the peak pullout resistance was evaluated through equations (8) and (13).

Table *3* shows the experimental peak pullout resistance (P_R^{Exp}) and theoretical one (P_R^{Theor}) calculated using the new proposed analytical method and the percentage differences between experimental results and theoretical values.

The differences between the predicted and the experimental values range from 1% to 38%, for GGR1, from 1% to 22% for GGR2, from 4% to 31% for GGR3 geogrid; from 1% to 11% for GGR4 geogrid.

Figure *7* shows, for each selected geogrid, the comparison between experimental and theoretical values of the peak pullout resistances, evaluated for different applied normal effective confining stresses. The comparison clearly shows the applicability of the proposed analytical method, efficiently predicting peak pullout resistances both for different applied vertical effective normal stresses and for different reinforcement lengths.

5 CONCLUSIONS

The paper deals with evaluating the peak pullout resistance of polymeric geogrids embedded in granular soils, considering interference phenomenon for closely spaced bearing members.

Based on the experimental results obtained by several pullout tests performed on different geogrids varying the specimen length and the applied vertical effective pressure, an upgrade of the theoretical method developed by Moraci and Gioffrè (2006) is proposed applying a interference reduction factor $C_{\alpha b}$.

The proposed analytical method can take into account the effects of: (i) soil dilatancy; (ii) reinforcement extensibility; (iii) geogrid geometry; (iv) vertical effective stress; (v) reinforcement length; (vi) interference phenomenon for closely spaced bearing members.

The validity of the solution was verified by comparison with experimental test results in terms of peak pullout resistance performed on four different PP biaxial geogrids.

The theoretical values obtained by the proposed model are consistent with the experimental data. Additional pullout tests will be carried out in order to extend the proposed method to other types of geogrids in contact with granular soils.

List of notation

α_s	Fraction of geogrid surface area that is solid (dimensionless)
δ	Mobilized skin friction angle between soil and geogrid (deg.)
σ'_b	Bearing stress (kN/m^2)
σ'_n	Normal effective stress (kN/m^2)
A_b	Area of each rib element (including the single node and the bar portion
A_r	Node embossment area (mm^2)
A_t	Bar portion between two nodes area (mm^2)
B_{eq}	Thickness of the equivalent uniform strip rib (mm)
B_R	Node thickness (mm)
B_T	Thickness of the rib portion between two nodes (mm)
$C_{\alpha S}$	Reduction coefficient of geogrid area where skin friction develops (-)
D_{50}	Average grain size (mm)
D_R	Relative density of soil (dimensionless)
$J_{2\%}$	Secant tensile stiffness at 2% strain (ISO 10319) (kN/m)
L_R	Specimen length (m)
n_t	Number of geogrid bearing members (-)
n_{tb}	Number of nodes in a transversal element (-)
P_R	Pullout resistance (kN/m)
P_{RS}	Skin friction component of pullout resistance (kN/m)
P_{RB}	Bearing component of pullout resistance (kN/m)
S	Spacing between geogrid bearing members (mm)
w_{opt}	Optimum water content (%)
W_B	Width of the bar (mm)
W_R	Node width (mm)
W_T	Width of the bar portion between two nodes (mm)
ϕ'_{CV}	Soil shear strength angle at constant volume (deg.)
ϕ'_P	Peak shear strength angle (deg.)
γ_{dmax}	Maximum dry unit weight (kN/m^3)

Tables

Table 1. Geometric properties of the geogrid used in this research.

Geogrid	polymer	Direction test	S [mm]	W_t [mm]	B_t [mm]	W_r [mm]	B_r [mm]	A_b [mm]	α_S [-]	B_{eq}/D_{50}^{A} [-]	B_{eq}/D_{50}^{B} [-]	S/B_{eq} [-]
GGR1	PP	TD	61,20	38,00	3,60	15,80	7,40	224,49	0,25	13,04	2,84	14,67
	PP	MD	53,80	46,00	1,85	15,20	7,40	133,74	0,25	6,83	1,49	24,62
GGR2	PP	TD	38,80	17,70	2,90	14,80	5,60	104,61	0,31	10,06	2,19	12,05
	PP	MD	32,50	31,80	1,90	7,00	5,50	78,62	0,31	6,33	1,38	16,04
GGR3	PP	TD	62,00	47,00	3,70	17,00	7,80	269,10	0,23	13,14	2,86	14,75
	PP	MD	64,00	53,00	2,20	9,00	7,80	151,70	0,23	7,65	1,66	26,16
GGR4	PP	TD	31,50	24,00	3,80	16,50	6,40	163,80	0,32	12,64	2,75	7,79
	PP	MD	40,50	25,50	2,00	6,00	6,50	66,00	0,32	6,55	1,43	19,33
GGR5	HDPE	TD	240,00	4,50	4,00	13,70	7,00	59,10	0,30	10,15	2,21	73,91
GGR6	HDPE	TD	240,00	4,40	4,50	15,20	6,80	83,64	0,36	13,34	2,90	56,24
GGR7	HDPE	TD	220,00	6,00	3,00	14,50	4,40	60,05	0,40	9,15	1,99	75,10

Table 2. Mechanical characteristics of the soils used.

	ϕ'_P [°]				ϕ'_{CV} [°]
	σ'_V=10 kPa	σ'_V=25 kPa	σ'_V=50 kPa	σ'_V=100 kPa	
Soil A	48	46	44	42	34
Soil B	52	50	47	44	37

Table 3. Theoretical and experimental peak pullout resistance values obtained in Soil A.

Geogrid	L_R	σ'_v	P_R^{Exp}	P_R^{Theor}	$\lvert P_R^{Exp} - P_R^{Theor}\rvert / P_R^{Exp}$
	[m]	[kPa]	[kN/m]	[kN/m]	[%]
GGR1	0.40	10	6,93	8,05	16,1
	0.90		17,57	17,48	0,5
	1.15		22,38	22,83	2,0
	0.40	25	14,61	15,47	5,9
	0.90		-	-	-
	1.15		-	-	-
	0.40	50	17,63	24,29	37,8
	0.90		-	-	-
	1.15		-	-	-
GGR2	0.40	10	9,39	6,92	26,3
	0.90		20,25	16,80	17,0
	1.15		22,92	20,69	9,7
	0.40	25	17,24	13,40	22,3
	0.90		35,82	32,47	9,3
	1.15		40,35	40,01	0,8
	0.40	50	23,78	21,22	10,8
	0.90		-	-	-
	1.15		-	-	-
GGR3	0.40	10	9,62	7,49	13,1
	0.90		19,58	18,62	4,9
	1.15		22,61	24,77	9,6
	0.40	25	15,04	14,39	4,3
	0.90		33,51	35,71	6,6
	1.15		36,26	46,47	30,9
	0.40	50	21,83	22,60	3,5
	0.90		-	-	-
	1.15		-	-	-
GGR4	0.40	10	7,93	7,28	8,2
	0.90		19,63	17,49	10,9
	1.15		22,08	22,32	1,1
	0.40	25	15,85	14,09	11,1
	0.90		31,96	33,80	5,7
	1.15		-	-	-
	0.40	50	21,26	22,31	4,9
	0.90		-	-	-
	1.15		-	-	-

Figures

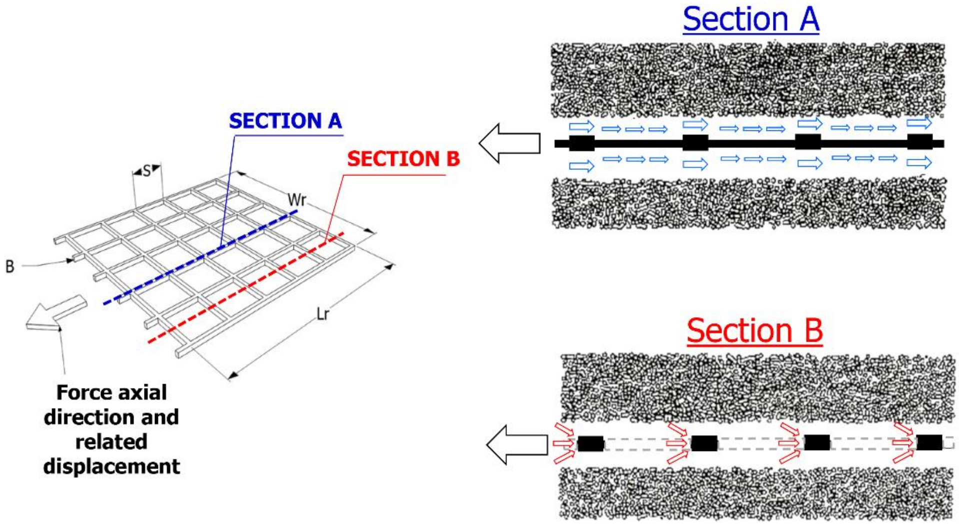

Figure 1: Schematic representation of grid geometry (Jewell et al., 1985)

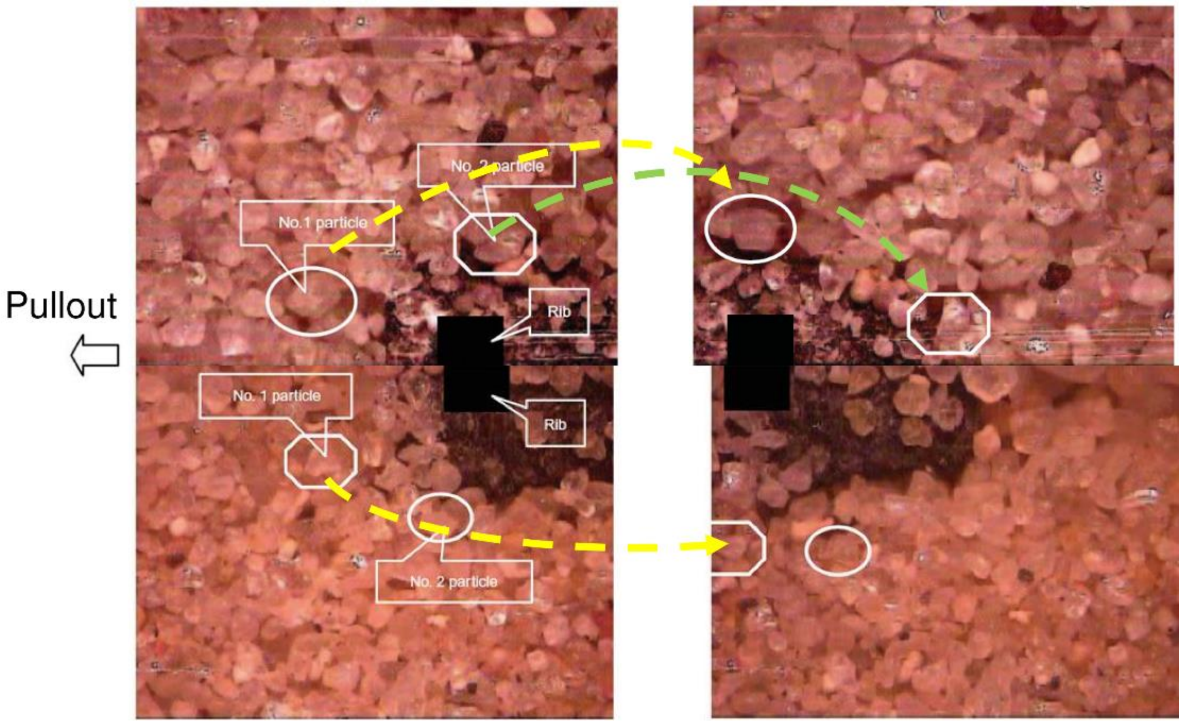

Figure 2. Particles motion around transverse rib (modified from Zhou et al. (2012))

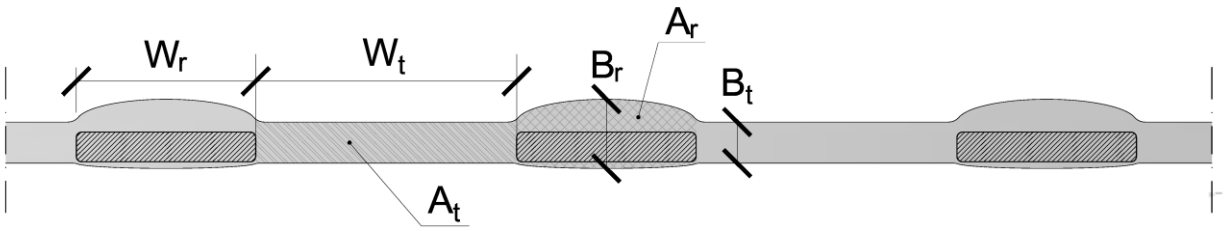

Figure 3. Schematic cross section of a generic transversal geogrid bar.

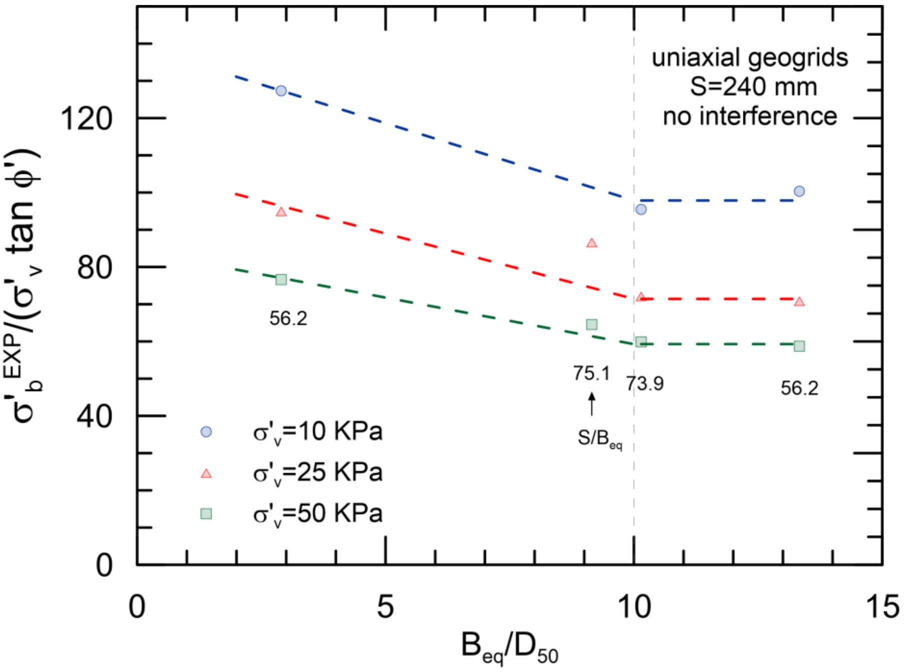

(a)

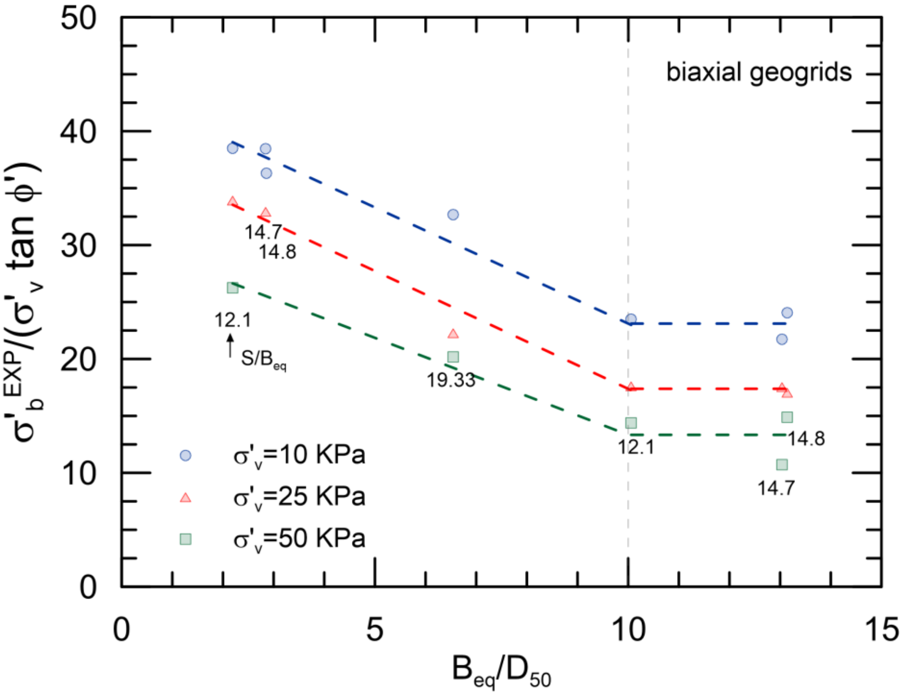

(b)

Figure 4. – Scale effect: results of pull-out tests in terms of $\sigma'_b/(\sigma'_v \tan\phi')$ ratio, carried out on different soils using (a) uniaxial geogrids in which interference effect is negligible and (b) biaxial geogrid with similar S/B_{eq} ratio (b).

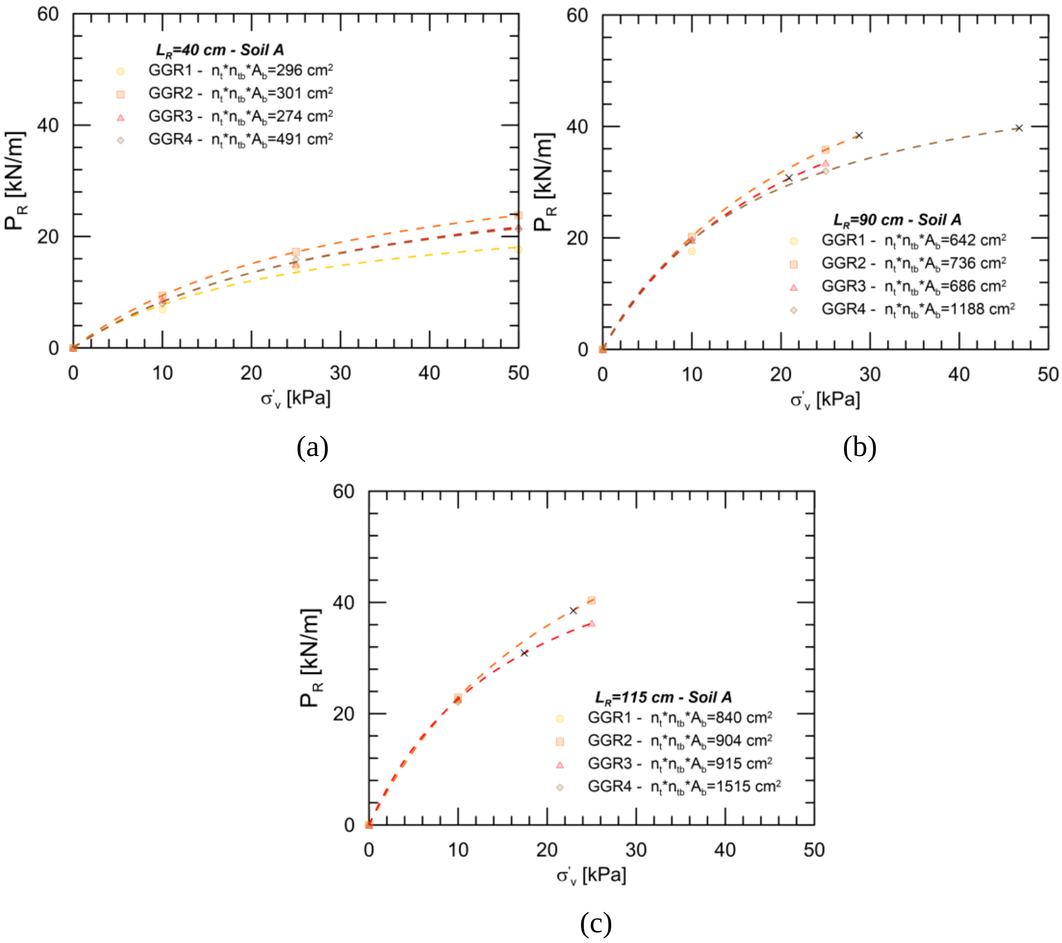

Figure 5. Peak pullout resistance envelope, for each anchorage length studied, varying the normal effective confining stress, obtained for GGR1 (a), GGR2 (b) and GGR3 (c).

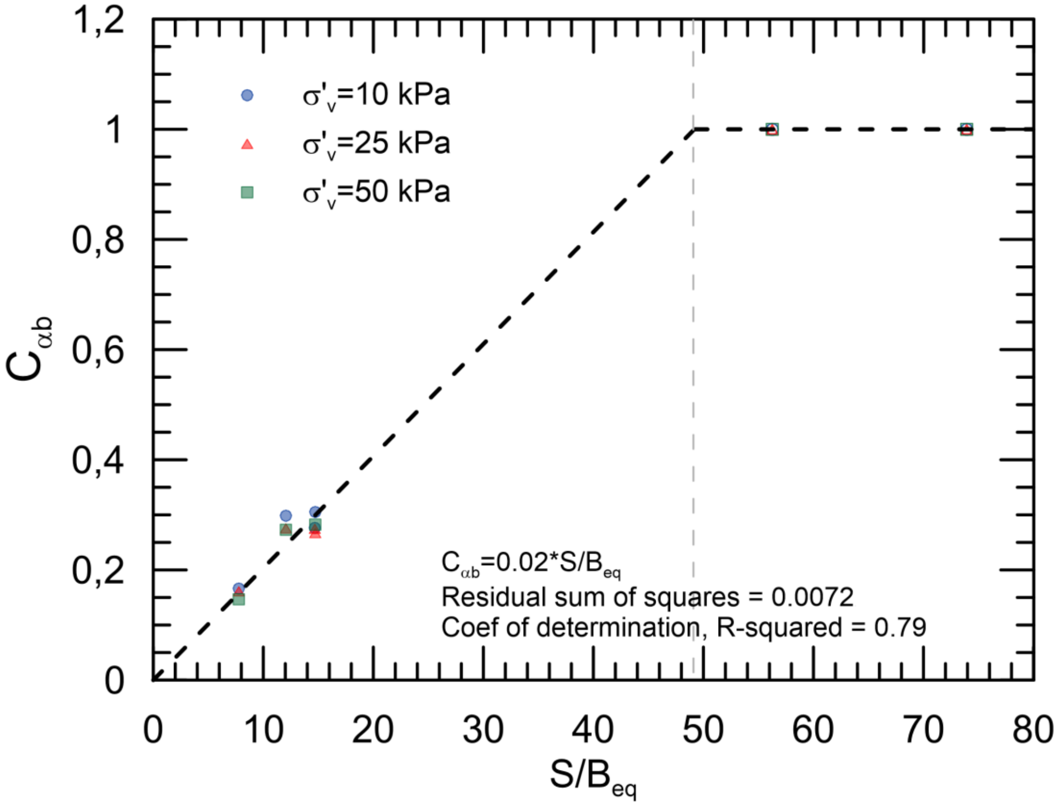

Figure 6. Variation of the reduction factor for the bearing resistance $C_{\alpha b}$ with the normalized spacing between transversal members S/B_{eq}.

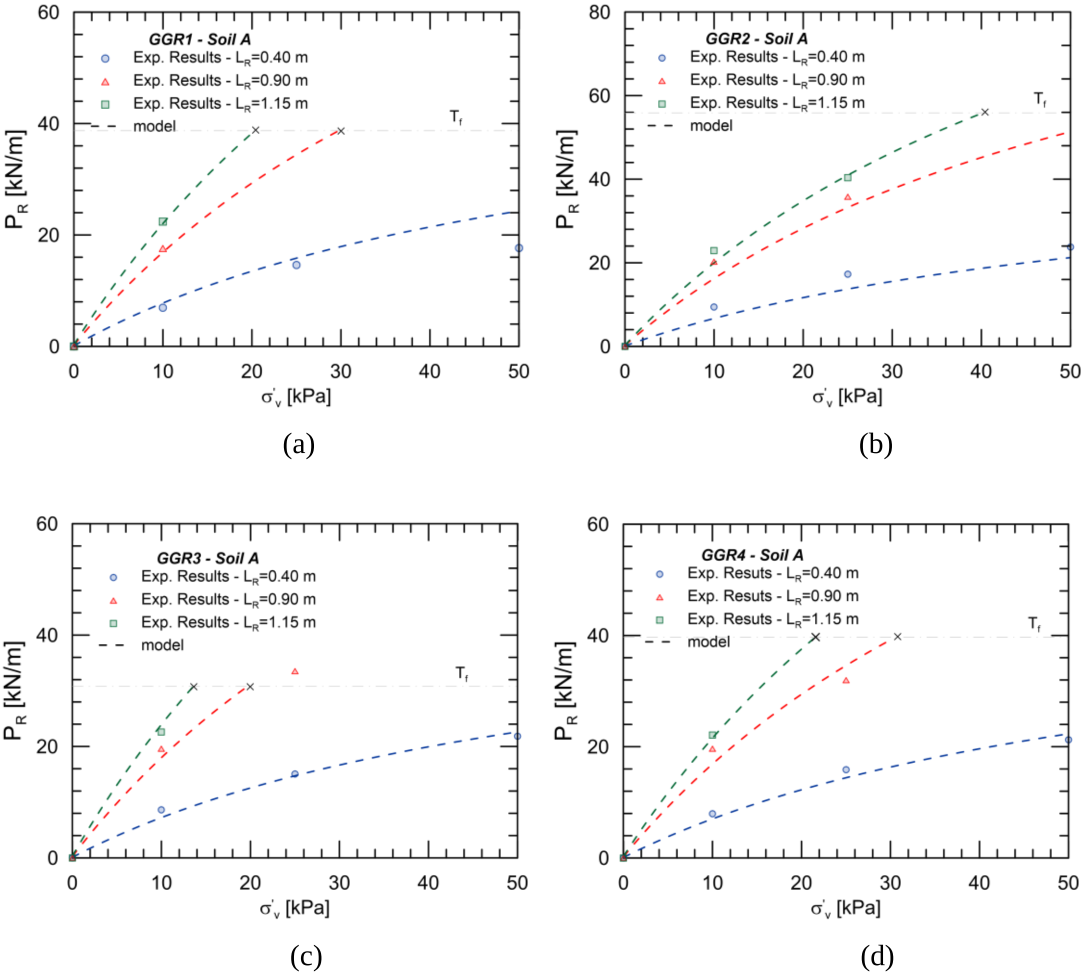

Figure 7. Comparison between experimental and theoretical values of peak pullout resistance regarding extruded bidirectional geogrid GGR1 (a), GGR2 (b) GGR3 (c) and GGR4 (d).

6 REFERENCES

Bathurst, R.J., Ezzein, F.M., 2015a. Geogrid and soil displacement observations during pullout using a transparent granular soil. Geotechnical Testing Journal 38 (5), 1-13.

Bathurst, R.J., Ezzein, F.M., 2015b. Geogrid pullout load–strain behaviour and modelling using a transparent granular soil. Geosynthetics International 23 (4), 271-286

Bergado, D.T., Chai, J.C., 1994. Pullout force/displacement relationship of extensible grid reinforcements. Geotextiles and Geomembranes 13 (5), 295-316.

Bergado, D.T., Shivashankar, R., Alfaro, M.C., Chai, J.-C., Balasubramaniam, A.S., 1993. Interaction behaviour of steel grid reinforcements in a clayey sand. Geotechnique 43 (4), 589-603.

Calvarano, L.S., Gioffrè, D., Cardile, G., Moraci, N., 2014. A stress transfer model to predict the pullout resistance of extruded geogrids embedded in compacted granular soils, 10th International Conference on Geosynthetics, ICG 2014, Deutsche Gesellschaft fur Geotechnik e.V., Berlin, Germany.

Cardile, G., Calvarano, L.S., Gioffrè, D., Moraci, N., 2014. Experimental evaluation of the pullout active length of different geogrids, 10th International Conference on Geosynthetics, ICG 2014, Deutsche Gesellschaft fur Geotechnik e.V., Berlin, Germany.

Cardile, G., Moraci, N., Calvarano, L.S., 2016. Geogrid pullout behaviour according to the experimental evaluation of the active length. Geosynthetics International 23 (2), 194-205.

Cardile, G., Moraci, N., Pisano, M., 2016. Tensile behaviour of a hdpe geogrid under cyclic loadings: experimental results and empirical modelling. Geosynthetics International. [http://dx.doi.org/10.1680/jgein.16.00019].

Cazzuffi, D., Calvarano, L.S., Cardile, G., Moraci, N., Recalcati, P., 2011. European experience in pullout tests: The influence of geogrid's geometry and structure on interface behaviour. Geosynthetics 29 (5), 42- 51.

Cazzuffi, D., Moraci, N., Calvarano, L.S., Cardile, G., Gioffrè, D., Recalcati, P., 2014. The influence of vertical effective stress and of geogrid length on interface behaviour under pullout conditions. Geosynthetics 32 (2), 40-50.

Dyer, M.R., 1985. Observations of the stress distribution in crushed glass with applications to soil reinforcement, Ph.D. Thesis, Magdalene College. University of Oxford, Michaelmas Term, p. 220.

Esfandiari, J., Selamat, M.R., 2012. Laboratory investigation on the effect of transverse member on pull out capacity of metal strip reinforcement in sand. Geotextiles and Geomembranes 35, 41-49.

Ezzein, F.M., Bathurst, R.J., 2014. A new approach to evaluate soil-geosynthetic interaction using a novel pullout test apparatus and transparent granular soil. Geotextiles and Geomembranes 42 (3), 246-255.

Fannin, J., Raju, D.J., 1993. Large-scale pull-out test results on geosynthetics, Geosynthetics '93, Vancouver, Canada, pp. 633-643.

Ferreira, F.B., Vieira, C.S., Lopes, M.d.L., 2015. Direct shear behaviour of residual soil–geosynthetic interfaces – influence of soil moisture content, soil density and geosynthetic type. Geosynthetics International 22 (3), 257-272.

Hatami, K., Esmaili, D., 2015. Unsaturated soil–woven geotextile interface strength properties from small-scale pullout and interface tests. Geosynthetics International 22 (2), 161-172.

Jacobs, F., Ziegled, M., Vollmert, L., Ehrenberg, H., 2014. Explicit design of geogrids with a nonlinear interface model, 10th International Conference on Geosynthetics, Berlin, Germany.

Jewell, R.A., 1990. Reinforcement bond capacity. Geotechnique 40 (3), 513-518.

Jewell, R.A., 1996. Soil Reinforcement with geotextile. CIRIA Thomas Telford, London.

Jewell, R.A., Milligan, G.W.E., Sarsby, R.W., Dubois, D., 1985. Interaction between soil and geogrids, in: Telford, T. (Ed.), Symposium on Polymer Grid Reinforcement in Civil Engineering, pp. 18-30.

Liu, C.-N., Ho, Y.-H., Huang, J.-W., 2009. Large scale direct shear tests of soil/PET-yarn geogrid interfaces. Geotextiles and Geomembranes 27 (1), 19-30.

Liu, F.-Y., Wang, P., Geng, X., Wang, J., Lin, X., 2016. Cyclic and post-cyclic behaviour from sand–geogrid interface large-scale direct shear tests. Geosynthetics International 23 (2), 129-139.

Matsui, T., San, K.C., Nabeshima, Y., Amin, U.N., 1996. Bearing mechanism of steel grid reinforcement in pullout test, International Symposium on Earth Reinforcement, Fukuoka, Kyushu, Japan, pp. 101-105.

Milligan, G.W.E., Earl, R.F., Bush, D.I., 1990. Observations of Photo-Elastic Pullout Tests on Geotextiles and Geogrids, 4th International Conference on Geotextiles, Geomembranes and Related Products, pp. 747-751.

Moraci, N., Cardile, G., 2008. Pullout behaviour of different geosynthetics embedded in granular soils, 4th Asian Regional Conference on Geosynthetics, Shanghai, China, pp. 146-150.

Moraci, N., Cardile, G., 2009. Influence of cyclic tensile loading on pullout resistance of geogrids embedded in a compacted granular soil. Geotextiles and Geomembranes 27 (6), 475-487.

Moraci, N., Cardile, G., 2012. Deformative behaviour of different geogrids embedded in a granular soil under monotonic and cyclic pullout loads. Geotextiles and Geomembranes 32, 104-110.

Moraci, N., Cardile, G., Gioffrè, D., 2007. A theoretical method to predict the pullout behaviour of extruded geogrids embedded in granular soils, 5th International Symposium on Earth Reinforcement, Fukuoka, Japan, pp. 281-287.

Moraci, N., Cardile, G., Gioffrè, D., Mandaglio, M.C., Calvarano, L.S., Carbone, L., 2014a. Soil Geosynthetic Interaction: Design Parameters from Experimental and Theoretical Analysis. Transportation Infrastructure Geotechnology 1 (2), 165-227.

Moraci, N., Cazzuffi, D., Calvarano, L.S., Cardile, G., Gioffrè, D., Recalcati, P., 2014b. The influence of soil type on interface behavior under pullout conditions. Geosynthetics 32 (3), 42-50.

Moraci, N., Gioffrè, D., 2006. A simple method to evaluate the pullout resistance of extruded geogrids embedded in a compacted granular soil. Geotextiles and Geomembranes 24 (3), 198-199.

Moraci, N., Recalcati, P., 2006. Factors affecting the pullout behaviour of extruded geogrids embedded in compacted granular soil. Geotextiles and Geomembranes 24 (4), 220-242.

Mosallanezhad, M., Alfaro, M.C., Hataf, N., Sadat Taghavi, S.H., 2016. Performance of the new reinforcement system in the increase of shear strength of typical geogrid interface with soil. Geotextiles and Geomembranes 44 (1), 457-462.

Palmeira, E.M., 1987. The study of soil-reinforcement interaction by means of large scale laboratory tests. University of Oxford, Trinity Term, Magdalen College.

Palmeira, E.M., 2004. Bearing force mobilisation in pull-out tests on geogrids. Geotextiles and Geomembranes 22 (6), 481-509.

Palmeira, E.M., 2009. Soil–geosynthetic interaction: Modelling and analysis. Geotextiles and Geomembranes 27 (5), 368-390.

Palmeira, E.M., Milligan, G.W.E., 1989. Scale and other factors affecting the results of pull-out tests of grid buried in sand. Geotechnique 39 (3), 511-524.

Perkins, S.W., 2000. Constitutive modeling of geosynthetics. Geotextiles and Geomembranes 18 (5), 273-292.

Peterson, L.M., Anderson, L.R., 1980. Pullout Resistance of Welded Wire Mats Embedded in Soil. Research Report Submitted to Hilfiker Co., pp. 106, from the Civil & Envir. Eng. Dept., Utah State Univ., Utah, USA.

Pinho-Lopes, M., Paula, A.M., Lopes, M.L., 2016. Soil–geosynthetic interaction in pullout and inclined-plane shear for two geosynthetics exhumed after installation damage. Geosynthetics International, 23 (5), 331-347.

Raju, D.M., 1995. Monotonic and cyclic pullout resistance of geosynthetic. Ph.D Thesis, University of British Columbia, Vancouver, Canada.

Sieira, A.C.C.F., Gerscovich, D.M.S., Sayao, A.S.F.J., 2009. Displacement and load transfer mechanisms of geogrids under pullout condition. Geotextiles and Geomembranes 27 (4), 241-253.

Sukmak, K., Sukmak, P., Horpibulsuk, S., Han, J., Shen, S.-L., Arulrajah, A., 2015. Effect of fine content on the pullout resistance mechanism of bearing reinforcement embedded in cohesive–frictional soils. Geotextiles and Geomembranes 43 (2), 107-117.

Suksiripattanapong, C., Horpibulsuk, S., Chinkulkijniwat, A., Chai, J.C., 2013. Pullout resistance of bearing reinforcement embedded in coarse-grained soils. Geotextiles and Geomembranes 36, 44-54.

Tran, V.D.H., Meguid, M.A., Chouinard, L.E., 2013. A finite e discrete element framework for the 3D modeling of geogrid-soil interaction under pullout loading conditions. Geotextiles and Geomembranes 37, 1-9.

Vangla, P., Gali, M.L., 2016. Effect of particle size of sand and surface asperities of reinforcement on their interface shear behaviour. Geotextiles and Geomembranes 44 (3), 254-268.

Vieira, C.S., Lopes, M.d.L., Caldeira, L.M., 2013. Sand-geotextile interface characterisation through monotonic and cyclic direct shear tests. Geosynthetics International 20 (1), 26-38.

Wang, Z., Jacobs, F., Ziegler, M., 2014. Visualization of load transfer behaviour between geogrid and sand using PFC2D. Geotextiles and Geomembranes 42 (2), 83-90.

Wang, Z., Jacobs, F., Ziegler, M., 2016. Experimental and DEM investigation of geogrid–soil interaction under pullout loads. Geotextiles and Geomembranes 44 (3), 230-246.

Zhou, J., Chen, J.-F., Xue, J.-F., Wang, J.-Q., 2012. Micro-mechanism of the interaction between sand and geogrid transverse ribs. Geosynthetics International 19 (6), 426-437.

Ziegler, M., Timmers, V., 2004. A new approach to design geogrid reinforcement, 3rd European Geosynthetics Conference Munich, Germany, pp. 661-665.

Figure captions